

Direct and Sensitized Photolysis of Phosphine Oxide Polymerization Photoinitiators in the Presence and Absence of a Model Acrylate Monomer: A Time Resolved EPR, Cure Monitor, and PhotoDSC Study

René M. Williams,^{†,§} Igor V. Khudyakov,[‡] Michael B. Purvis,[‡] Bob J. Overton,[‡] and Nicholas J. Turro^{*,†}

Department of Chemistry, Columbia University, New York, New York 10027, and Alcatel Telecommunications Cable, Claremont, North Carolina 28610

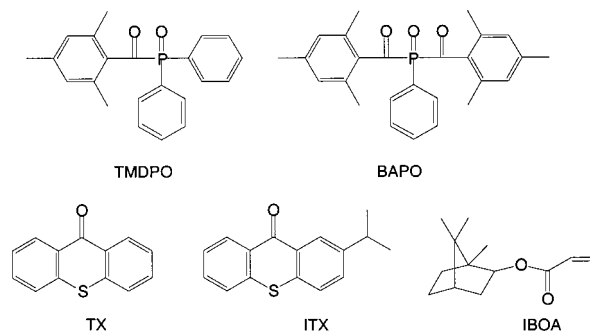
Received: April 7, 2000; In Final Form: August 21, 2000

The effect of triplet sensitizers on the photoinitiated polymerization (cure) of a model acrylate monomer, isobornyl acrylate (IBOA), has been investigated. Time-resolved electron paramagnetic resonance (TR EPR) spectroscopy was employed to investigate the initiation of polymerization. Cure monitoring and photodifferential scanning calorimetry (photoDSC) were employed to follow the course of the polymerization. Thioxanthene-9-one (TX) and 2-isopropylthioxanthene-9-one (ITX) were found to be effective sensitizers of the photopolymerization, which was initiated by radicals produced from (2,4,6-trimethylbenzoyl)diphenylphosphine oxide (TMDPO) and bis(2,4,6-trimethylbenzoyl)phenylphosphine oxide (BAPO). TR EPR experiments demonstrated that the mechanism of sensitization involves T–T energy transfer from TX (or ITX) to TMDPO or BAPO followed by formation of radicals by α -cleavage of the photoinitiators. Direct photolysis of TMDPO and BAPO results in an absorptive chemically induced dynamic electron polarization (CIDEP) pattern due to the triplet mechanism (TM) of polarization of the substituted benzoyl and P-centered radicals produced by α -cleavage of the photoinitiators. TR EPR demonstrates that the same radicals were produced during direct and sensitized photolysis. However, a different CIDEP pattern is produced by photosensitization, namely an emissive/absorptive (E^*/A) pattern. A TR EPR study of solutions containing phosphine oxide initiators and IBOA under direct and photosensitized conditions demonstrated that the polarized primary P-centered radicals add to the double bond of IBOA with the formation of polarized secondary radical adducts. Both primary and secondary radicals exhibit the same polarization pattern as the primary radical precursors, i.e., A in direct photolysis and E^*/A in the presence of a sensitizer. The rate of polymerization of neat IBOA was followed by cure monitoring. In the presence of ITX the rate of cure increases significantly compared to direct photolysis of same. The heat evolved in the polymerization of IBOA photoinitiated (direct and sensitized) with TMDPO was monitored by photoDSC, and at early times was found to be higher in the sensitized photopolymerization. Time-intermittent UV irradiation allowed an estimation of the ratio of termination to propagation rate constants (k_t/k_p) during dark periods of polymerization. The observed decrease of k_t/k_p with the progress of polymerization is discussed. The results suggest that photosensitization may provide a means of manipulating and controlling the parameters of photocuring of acrylates.

1. Introduction

Phosphine oxides such as (2,4,6-trimethylbenzoyl)diphenylphosphine oxide (TMDPO) and bis(2,4,6-trimethylbenzoyl)phenylphosphine oxide (BAPO) (cf. Chart 1 below) are widely used as photoinitiators in the coating industry.^{1–3} There are a number of reasons for the attractiveness of phosphine oxides as photoinitiators: (1) their good UV absorption, (2) their high quantum yield of photodissociation into benzoyl and phosphinoyl radicals which initiate polymerization, (3) the high reactivity of the photoproducted radicals toward addition to acrylate monomers, and (4) their ability to cure thick films.^{1,4–6} The overall speed and efficiency of a photocure is very important in practical applications. Photosensitization provides a possible means of increasing the overall speed and efficiency of

CHART 1



photocuring. For example, the combination of α -morpholinoketone photoinitiators and sensitizers of thioxanthene-9-one (TX) family has been reported to lead to an increase in the rate of cure.^{7,8} The use of TXs as photosensitizers of radical formation from phosphine oxides, a possible means of increasing the

[†] Columbia University.

[‡] Alcatel Telecommunications Cable.

[§] Present address: Instituut voor Moleculaire Chemie, University of Amsterdam, Nieuwe Achtergracht 166, 1018 WV Amsterdam, The Netherlands.

efficiency of photopolymerization or photocure of acrylates, is the subject of this report.

We report an investigation of direct and TX and 2-isopropylthioxanth-9-one (ITX) sensitized photolysis of TMDPO and BAPO in the presence and absence of a model acrylate monomer, isobornyl acrylate (IBOA), which is widely used in commercial coatings as a reactive diluent. The structures of the compounds used in this work are shown in Chart 1.

In order to obtain information on both the initial stages of the polymerization (photochemical formation of radicals from photoinitiator and addition of photoinitiator radicals to monomer) and the crucial polymerization stages (propagation and termination of polymerization), several techniques were employed and direct and sensitized initiation of polymerization were compared. In particular, we have employed continuous wave time-resolved EPR (TR EPR) to monitor directly the first steps of the photoinitiated polymerization of IBOA, as a model monomer which is widely employed as a reactive diluent in the coating industry. In addition, we have employed a cure monitor technique to measure the cure speed and photo differential scanning calorimetry (photoDSC) to monitor the kinetics of the formation of polymer.

2. Experimental Section

2.1. Materials. The following reagents and solvents were used as received: 2,4,6-trimethylbenzoyl)diphenylphosphine oxide (TMDPO) from BASF; 2,4,6-bis(trimethylbenzoyl)phenylphosphine oxide (BAPO) from Ciba Additives; thioxanth-9-one (TX), benzophenone, benzil (all three from Aldrich); isopropylthioxanth-9-one (ITX) from First Chemical, or from Ciba. Commercial ITX is a mixture of 2- and 4-isopropyl TX; the latter isomer is the minor component. HPLC grade ethyl acetate (Aldrich) was used as a solvent in EPR experiments. Prior to its use, isobornyl acrylate (IBOA, Aldrich) was purified with column chromatography to remove any inhibitor.³

2.2. Techniques and Measurements. The TR EPR equipment is described in detail elsewhere.^{5,9} The instrument consists of a Bruker ER 100D X-band spectrometer, PAR boxcar integrator and signal processor (model 4402). A rectangular thin quartz flow cell was used; flow rates were typically between 0.7 and 1.7 mL/min. Freshly prepared solutions were used throughout. In the TR EPR experiments, solutions were deoxygenated by prolonged bubbling with argon. Solutions for TR EPR had an optical density of 0.3–0.5 at the optical path of 0.3 mm, the thickness of the EPR cell. Solutions were excited in the EPR cavity with Spectra Physics GRC 150 Nd:YAG laser (λ 355 nm, pulse duration 10 ns, frequency 30 Hz, energy 20 mJ/pulse).

The speed of the cure was monitored with a CM 1000 Cure Monitor (Spectra Group Ltd.). The measurements were performed as described elsewhere.³

A Perkin-Elmer photoDSC DPA-7 was employed to monitor the heat produced during polymerization. An Osram Hg 100 W lamp was used as the light source. Samples on a DSC pan were flushed with nitrogen for 10 min prior to irradiation. All photoDSC experiments were performed at 50 °C. The mass of samples was 3–4 mg. At least five experiments were performed with one solution under the same conditions, and the average values were recorded. Most of the experiments were run with the full light of the lamp with UV-light of intensity of 20 mW/cm² measured with a radiometer/photometer (International Light). Irradiations with the full light of the different intensities (0.2–40 mW/cm²) or with UV light passed through the

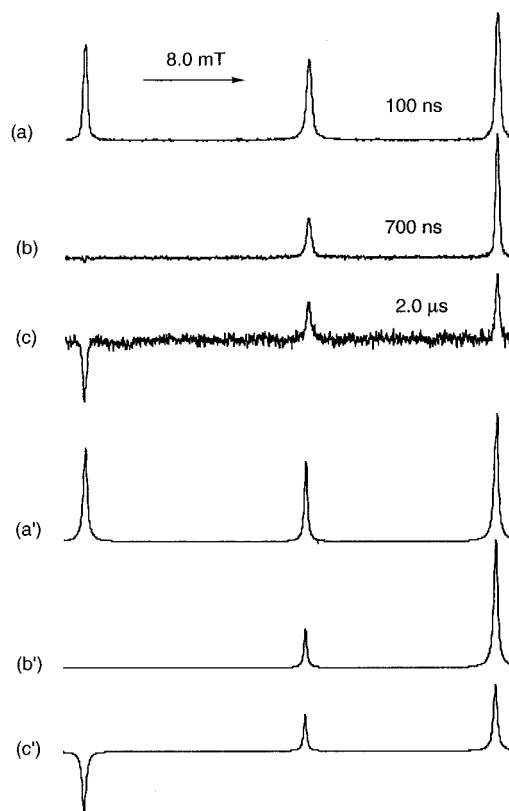


Figure 1. TR EPR spectra of TMDPO (2.4×10^{-2} M) in ethyl acetate taken at different times and computer-simulated spectra: (a) 100–200 ns; (b) 700–1000 ns; and (c) 2000–5000 ns following laser excitation (355 nm). The simulated spectra are a mixture of TM and RPM mechanisms. See text for discussion.

monochromator were performed as well. In particular, we irradiated IBOA solutions with light of λ 385 nm (5.8 mW/cm²).

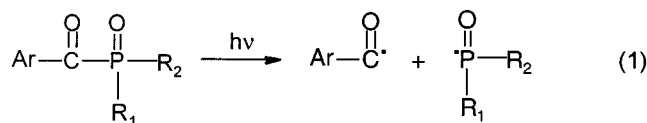
The consumption of IBOA during photoDSC measurements was monitored by IR spectroscopy. IR spectra (ATR FT IR, Nicolet Magna-IR 550) of IBOA solutions of TMDPO were taken *before* cure; the acrylate group intensity at ~ 810 cm⁻¹ relative to intensity of carbonyl or alkyl (C–H) vibrations was measured to determine conversion. A sample with a mass of a few milligrams taken out of a DSC pan was employed to take IR spectra of samples *after irradiation* in photoDSC measurements. The decrease of the (relative) intensity of acrylate group was used as a measure of IBOA conversion (ξ). IR spectra were taken at two opposite sides of an irradiated IBOA thin layer in a DSC pan. The difference in ξ measured in two ways was within the experimental uncertainty of determining ξ . At least five measurements were performed. IgorPro 3.12 software was used to analyze the kinetic analysis related to DSC traces.

Solutions of TMDPO at concentrations of 2.3×10^{-2} to 8.2×10^{-2} M (0.8–2.9%) in the neat IBOA were used in photoDSC experiments. In the experiments involving photosensitizer, ITX was added to TMDPO solutions in IBOA; the range of [ITX] was 8.0×10^{-3} – 4.5×10^{-2} M.

3. Results and Discussion

3.1. Direct Photolysis of TMDPO and BAPO. Figure 1 presents TR EPR spectra of TMDPO in ethyl acetate. Quite similar spectra were observed^{9–13} and analyzed¹² earlier. Acyl and bis(acyl)phosphine oxides such as TMDPO and BAPO undergo efficient photolysis (α -cleavage) via the triplet state to produce substituted benzoyl (referred to as benzoyl for the remainder of this report) and phosphorus centered radicals as

shown in eq 1:^{9–13}



Two mechanisms of CIDEP are usually considered to be responsible for the most common polarization patterns observed for radicals produced by photolysis in homogeneous solutions: the triplet mechanism (TM) and the S–T₀ radical pair mechanism (RPM).^{9–13} In systems involving radical pairs possessing very large hyperfine coupling (HFC) constants, a third mechanism, S–T_{RPM} is sometimes invoked.¹⁴ The absorptive (CIDEP pattern of the spectrum of TMDPO at the early time of observation (Figure 1) is known to be due to a dominant action of TM which leads to new enhanced absorption (enhanced absorption signified as A, emission signified as E throughout).^{9–12} We obtained a value of $a_P = 36.2$ mT for the hyperfine coupling constant of phosphorus-centered radical produced from photolysis of TMDPO (cf. eq 1) in ethyl acetate (Figure 1). Direct photolysis of BAPO also resulted in a CIDEP pattern (similar to that of Figure 1 and to TR EPR reported¹⁹ earlier). We obtained $a_P = 25.6$ mT for the hyperfine coupling constant of the phosphorus-centered radical produced from photolysis of BAPO (cf. eq 1) in ethyl acetate.

At later times of spectrum observation, both TMDPO and BAPO show a contribution of RPM with an emissive-absorptive (E/A)^{20,21} CIDEP pattern of the spectrum of the phosphorus-centered radical becoming evident (Figure 1 shows the results for TMDPO). Also, Figure 1 presents computer simulations¹⁵ of the corresponding TR EPR spectra. All simulations made in this work include only CIDEP contributions from TM and RPM.¹⁶ The simulation demonstrates that a contribution of the RPM (15%) is observed even at the earliest times of observation (Figure 1).¹⁷ No contribution of the S–T_{RPM} mechanism was invoked.

Although the phosphorus-centered radicals show E/A polarization at later times, the benzoyl radical (eq 1) appears as a relatively broad absorptive signal^{9–13,18} in the center of the spectrum, even at later times of observation (Figure 1). The proton HFC constants of benzoyl radicals are small, and the overlap of unresolved hyperfine components causes the broadness of the signal.¹⁸

3.2. TX- and ITX-Sensitized Photolysis of TMDPO and BAPO. Photolysis of TMDPO or BAPO in the presence of photosensitizers TX or ITX results in similar TR EPR spectra at early and later times of observation. Representative spectra of TX-sensitized photolysis of TMDPO at early times and of the ITX-sensitized photolysis of a mixture of TMDPO and BAPO (mixtures of photosensitizers are representative of the practice in commercial photocuring) at later times are shown in Figure 2, a and b, respectively.

The CIDEP patterns for direct (Figure 1) and sensitized (Figure 2) photolysis of the phosphine oxide are very different. At early times and later times both the phosphorus-centered radicals show an E*/A pattern.^{20,21} The benzoyl radical shows an E (or E*/A) pattern. In the case of the photolysis of a mixture of TMDPO and BAPO (Figure 2b), the signals of two P-centered radicals are observed ($a_P = 25.6$ and 36.2 mT).¹⁴ It is clear that sensitized photolysis wipes out the TM of CIDEP, which leads to strong absorptive signals of TMDPO and BAPO. TR EPR signals are weaker (i.e., S/N ratio is lower) in the case of the sensitized photolysis, cf. Figures 1 and 2.

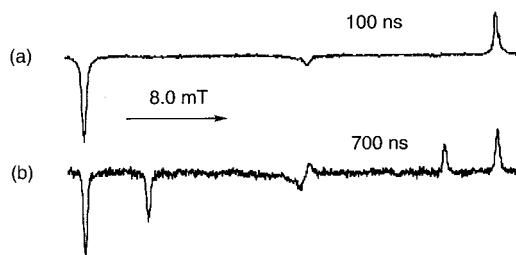


Figure 2. TR EPR spectra in ethyl acetate of (a) TMDPO (2.4×10^{-2} M) in the presence of TX (0.04 M) recorded 100–200 ns following excitation; (b) a mixture of TMDPO (4.8×10^{-3} M) and BAPO (2.4×10^{-3} M) in the presence of ITX (2.6×10^{-2} M) recorded 700–1000 ns following laser excitation.

The E*/A pattern of TR EPR spectra produced in the sensitized photolysis is consistent with the predominant action of RPM of CIDEP for photolysis via the triplet state of the phosphine oxides.^{20,21} Thus, we conclude that triplet–triplet (T–T) energy transfer from ITX or TX to TMDPO or BAPO takes place after photoexcitation of TMDPO or BAPO leading to the corresponding triplets of the phosphine oxides. The latter triplets then cleave into benzoyl and P-centered radicals. The E_T of TMDPO and BAPO (255–263 kJ/mol⁶) are lower or very close to the reported triplet energies of the sensitizers ($E_T = 262$ – 265 kJ/mol²²), both of which possess relatively long triplet lifetimes.⁶

Control experiments showed that no TR EPR signals were produced by photoexcitation of TX or ITX in the absence of TMDPO and BAPO.

T–T energy transfer from TX to TMDPO has been observed with laser flash photolysis.⁶ To provide further evidence for T–T energy transfer, we have studied the effect of the triplet energy of sensitizers on the CIDEP produced during photolysis of TMDPO. Benzophenone-sensitized photolysis results in the E*/A CIDEP pattern similar to that resulting from TX (or ITX) as sensitizer. Benzophenone has a triplet energy level ($E_T = 275$ kJ/mol²³) which is higher than both TMDPO or BAPO (255–263 kJ/mol⁶). However, benzil, with a low $E_T = 223$ kJ/mol,²³ did not sensitize the generation of polarization. Thus, the ability of a sensitizer to generate CIDEP from TMDPO or BAPO depends on the triplet energy of the sensitizer, as is expected in the case of triplet energy transfer. Such experiments convincingly demonstrate that T–T energy transfer occurs between thioxanthene-9-one sensitizers and the phosphine oxide initiators.

It has been established that TX (ITX) can serve as photoinitiators in the presence of hydrogen/electron donors, e.g., amines.^{7a,8} The observation of photosensitization of phosphine oxides by TX (ITX) is not trivial for at least two reasons: (1) the triplet energy levels of the sensitizers and phosphine oxides are close (vide supra) so that efficient energy transfer is not guaranteed and (2) the quantum yield of formation of triplets from TX has been shown to be less than unity and solvent dependent.^{7b} Nevertheless, the observations suggest that photosensitization is efficient under the conditions reported.

We comment on some of the features of the CIDEP spectra produced by photosensitization. The presence of an emissive component in the phosphorus radical CIDEP (Figure 2) is probably due to a S–T_{RPM} mechanism.^{20,21} We estimate a contribution of the E component to be 10%. The action of a S–T_{RPM} mechanism has been reported to be responsible for the CIDEP pattern of P-centered radicals demonstrating very large (hundreds of gauss) a_P values.¹⁴ A contribution of the S–T_{RPM} mechanism into CIDEP of phosphinoyl radicals was clearly observed for hydrogen abstraction from the correspond-

ing phosphites.¹⁴ Interestingly, the emissive component assigned to the $S-T_1$ mechanism is observed at the earliest times of spectrum detection (Figure 2a), and operates in a nonviscous solvent. The radical triplet pair mechanism (RTPM) could also result in an emissive contribution to CIDEP of radicals,^{20,21} although we do not believe it to be important here because of the rapid quenching of the triplet sensitizers by $T-T$ transfer at the concentrations of BAPO and TMDPO employed.

The weakness of the benzoyl radical signals (Figure 2) makes the interpretation of the CIDEP pattern difficult. However, the observed E/A or E^*/A CIDEP pattern, especially at latter times, is consistent with RPM,^{20,21} cf. Figure 2b. Due to poor spectral resolution of the hyperfine components of the benzoyl radical, the E/A pattern is apparently masked by the residual A polarization in the direct photolysis at later times (Figure 1b). There appears to be an emissive contribution due to $S-T_1$ mechanism into CIDEP of substituted benzoyl radical (cf. Figure 2) as well as in the CIDEP of P-centered radicals in the sensitized experiments. This emissive contribution results in the observed E (or E^*/A) (Figure 2a) and E/A (Figure 2b) pattern of the benzoyl radical.

A final comment addresses the effect of the difference between the g factors of substituted benzoyl ($g = 2.000^{10,12}$) and phosphinoyl radicals of TMDPO ($g = 2.003^{10,12}$) on the observed polarization. Not only HFC, but also Δg , contributes to $S-T_0$ evolution of the radical pair (RP) and the polarization coefficients of components in TR EPR spectrum.^{15,20} The Δg term adds an A component to the spectrum of a radical of the triplet RP with smaller g factor (benzoyl) and an E component to a radical with a larger g -factor (phosphinoyl). The contribution of the Δg term into polarization coefficients of these two radicals is thus qualitatively different. The Δg contribution is negligible (less than 2%) for the phosphinoyl radical because of its very large HFC constant; however, the Δg and HFC terms may make a similar contribution in the case of the substituted benzoyl radical which possess small HFC constants.^{11,15} Thus, the substituted benzoyl radical demonstrates an E- or E/A- pattern (cf. Figure 2) due to the predominant action of $S-T_1$ and RPM mechanisms despite the presence of an A component due to the Δg mechanism.

3.3. Direct and TX-Sensitized Photolysis of TMDPO in the Presence of an Acrylate Monomer, IBOA. Figure 3 presents the TR EPR spectra obtained during direct and TX-sensitized photolysis of TMDPO, both photolyses in the presence of IBOA. Similar results were observed for the TX-sensitized photolysis of BAPO in the presence of IBOA. The observed spectra consist mainly of polarized signals of the spin adducts of phosphinoyl radical and acrylate (Chart 2).

In direct photolysis the CIDEP of the spin adducts is A, and in the sensitized photolysis, the CIDEP is E/A. The weak outermost components in the spectra (Figure 3) are the residual signals of the phosphinoyl radical; the signals become indistinguishable from the noise at $t \sim 1 \mu\text{s}$. Comparison with Figures 1 and 2 shows that the polarization of the primary radicals (A in direct photolysis and E/A in sensitized photolysis) is transferred to the secondary adduct radicals.

Simulated spectra of the adducts (Figure 3, a' and b'), which reflect the main features of experimental spectra, are presented below the corresponding experimental spectra in Figure 3 and lead to the following HFC constants: $a_P = 5.94$, $a_{\alpha-H} = 1.71$, and $a_{\beta-H} = 1.96$ mT. These constants were used in the simulation of TR EPR spectra of spin-adducts (Figure 3) and are in agreement with the reported values for radical adducts to double bonds.^{4,24,25}

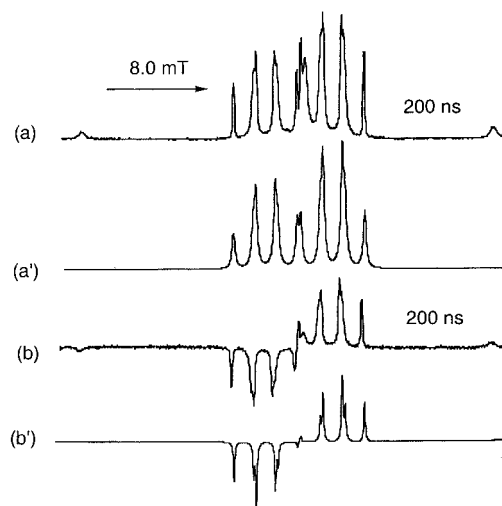
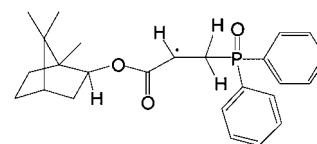


Figure 3. TR EPR spectra in ethyl acetate of (a) TMDPO (2.9×10^{-2} M) in the presence of IBOA (1.9 M); (b) TMDPO (2.4×10^{-2} M) in the presence of TX (0.04 M) and IBOA (1.6 M). Both spectra are recorded 200–800 ns following laser excitation. Computer-simulated spectra are also shown below the experimental spectra. See text for discussion.

CHART 2



The line width of the TR EPR of the spin adducts shows an alternation (Figure 3). In particular, the outermost components of the multiplets are narrower than the inner components. Such line width variations are known and have been discussed elsewhere.²¹ In the simulations a constant line width was employed.

Phosphinoyl radicals are very reactive toward double bonds.^{4,9,13,19} Thus, it is not surprising that TR EPR spectra in systems containing IBOA (Figure 3) result primarily from addition of phosphinoyl adducts (Chart 2) at the earliest acquisition times. Benzoyl radicals are much less reactive than phosphinoyl radicals toward addition to acrylates,^{4,9,13} and they persist, contributing to signals in the center of the spectra (Figure 3); cf. discussion in this section above. In accordance with the literature data,²⁶ “tail” adducts of radicals to IBOA are observed (Chart 2). The rate constant of a “head” addition is usually significantly lower than the rate constant of “tail” addition,²⁶ and “head” adducts are not observed within the limits of our simulations.

A recent TR EPR study on photoinduced reactions in the presence of acrylates claims that polarized vinyl radicals were formed by hydrogen abstraction of vinyl hydrogens from acrylate by triplet acetone in the presence of 2-propanol.²⁷ This is an unexpected result based on the high bond dissociation energy of vinyl C–H bonds. The satisfactory correspondence between the simulated and experimental TR EPR spectra (Figure 3) clearly represent addition of free radicals to acrylate and do not require the involvement of vinyl radical formation.

3.4. Effect of ITX on the Rate of Polymerization. Figure 4 presents the profiles of the rate of photocure of IBOA by TMDPO in the presence and absence of ITX. The rate of the photocure is strongly affected by the presence of a triplet sensitizer and is clearly faster. These data clearly demonstrate that the presence of the triplet sensitizer ITX significantly

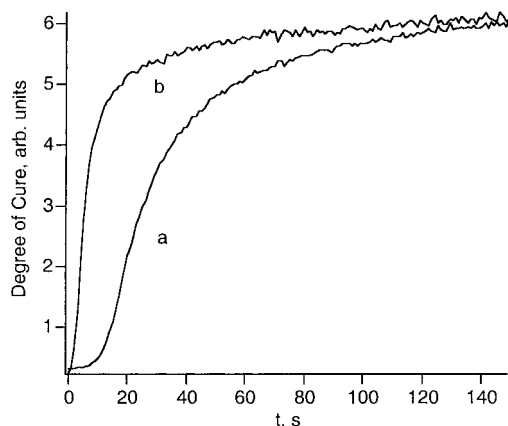


Figure 4. Cure monitoring profiles of the polymerization of IBOA with TMDPO (2.4×10^{-2} M) as photoinitiator in the absence (a) and in the presence (b) of ITX (0.04 M).

accelerates the speed of the polymerization (Figure 4). In control experiments with solutions containing ITX and IBOA, photolysis did not produce any polymerization within experimental error of the thermal control.

3.5. Photopolymerization of IBOA Initiated by TMDPO.

Formation of a spin adduct (Chart 2) is the initiation step of polymerization of IBOA. Polymerization of neat acrylates provides an established method for the curing of acrylate coatings.^{1,2} The problems related to the kinetics of photopolymerization of neat acrylates have been outlined elsewhere.³

Information on the features of the polymerization of IBOA with TMDPO as photoinitiator was obtained through the use of photoDSC, a technique that allows the direct measurement of heat produced in the polymerization as a function of the light dose delivered to the sample. Analysis of the heat profiles produced provides information on the parameters involved in the photoinduced polymerization.

Traditionally, polymerization is described as a chain reaction with a set of rate constants of elementary reactions among which (in the absence of significant chain transfer) the most important are the bimolecular steps of propagation (k_p) and termination (k_t). Formation of a polymer and vitrification of an acrylate solution during polymerization significantly changes properties of a medium undergoing polymerization. As a result, it is doubtful whether the standard eq 2 for the rate of polymerization R can be applied.^{3,28}

$$R = -d[M]/dt = (\omega_{in})^{1/2} k_p k_t^{-1/2} [M] \quad (2)$$

where ω_{in} is the rate of initiation of polymerization and $[M]$ is the molar concentration of a monomer.^{3,28} (Here and below we use k_t for brevity instead of $2k_t$). To interpret the experimental data, we consider the use of time (or conversion ξ)-dependent k_p and k_t for monofunctional acrylates.²⁷ Different experimental dependencies of R or ξ vs. time, light intensity, temperature, etc., have been obtained and discussed for many mono- and multifunctional acrylates.^{3,28} Our analysis involves the use of photoDSC in the determination of the dimensionless k_t/k_p ratio during polymerization, an approach we shall show provides useful information on the photopolymerization. From formal kinetics eq 3 may be derived for dark or post polymerization, i.e., polymerization after termination of photoinitiation:²⁸

$$[M]_t/R_t - [M]_0/R_0 = (k_t/k_p)t \quad (3)$$

In eq 3 $[M]_0$ (R_0) is the monomer concentration (rate of polymerization) at the beginning ($t = 0$) of dark polymerization

TABLE 1: Results of a PhotoDSC and IR Study of Polymerization IBOA under TMDPO (2.4×10^{-2} M) by Full Light

irradiation	Q , J/g ^a	ξ ^c	k_t/k_p ^d
60 s	312 ^b	0.97 ± 0.03	
5 pulses of 0.6 s each	228	0.70 ± 0.07	95; 45; 30; 25; 20 ^e
3 s	139	0.50 ± 0.05	50

^a Determination error is ± 5 J/g. ^b This is Q_{tot} . ^c Determined by IR. ^d Determination error is 10%. ^e For consecutive pulses $N = 1, 2, \dots, 5$.

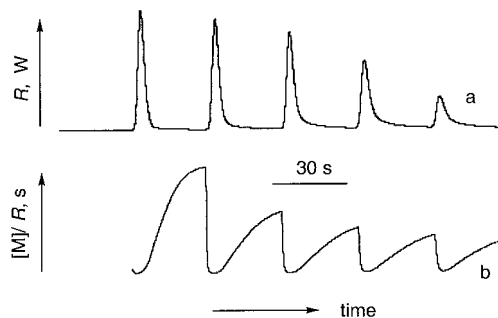


Figure 5. (a) PhotoDSC trace obtained during polymerization of TMDPO (2.4×10^{-2} M) in IBOA; (b) Calculated ratio of $[M]/R$ vs time of polymerization, see text.

monitoring; $[M]_t$ and R_t are the current concentration and rate, respectively. Equation 3 can be used to determine k_t/k_p (which is assumed to be constant during the limited range of conversions, ξ).

We determined k_t/k_p at different conversions ξ as follows. IR spectra show that photoirradiation of TMDPO in IBOA for 1 min with full light results in the complete consumption of IBOA, and in the formation of a solid polymer, cf. Table 1. The total heat, Q_{tot} , during complete polymerization is presented in Table 1. A release of heat during polymerization up to Q_{tot} can be identified with a decrease of concentration of IBOA from initial $[M]_{tot}$ to 0.

Figure 5a presents DSC traces observed during irradiation of solution of TMDPO in IBOA with five short light pulses ($N = 1-5$). The duration of each pulse is 0.6 s, with 30 s between pulses. The photoDSC trace presents the rate of polymerization dQ/dt (watts) = R .^{3,28,29} Most of the observed trace is dark polymerization, lasting 10–20 s after a light pulse; cf. Figure 5a. Integration of the DSC traces over t allows an estimation of the heat released during polymerization, $Q = Q(t)$ (joules). Figure 5b presents the time-dependent ratio $(Q_{tot} - Q)/[dQ/dt]$ (seconds). The latter ratio should be equal to $[M]/R$. We analyzed five ascending parts of a curve in Figure 5b, corresponding to five descending parts of a photoDSC trace of Figure 5a.

We fit each of the ascending parts of a curve of Figure 5b into the linear law.³⁰ A tangent of each linear fit was identified with k_t/k_p , cf. eq 3. The values of k_t/k_p obtained (values for pulses with $N = 1-5$) are presented in Table 1. We found that k_t/k_p decreases with N for $N \leq 5$ in this experiment, and in other experiments with different light intensities, full or monochromatic light, and different TMDPO concentrations. Estimations of k_t/k_p become less reliable for pulses with $N \geq 6$ due to the relatively small amount of released heat.

In the same way, the value of k_t/k_p was estimated after irradiation for 3 s (Table 1). The conversion ξ of IBOA was estimated (Table 1) by IR (cf. the Experimental Section) after the five pulses (Figure 5) and after one pulse with a duration equal to the total duration of irradiation with five pulses (3 s). Most of the IBOA is polymerized after irradiation with five

pulses, and the conversion is significantly higher than after continuous irradiation for 3 s. Most probably, both continuous and time-intermittent irradiation for 3 s result in the same amount (concentration) of photogenerated free radicals. Time-intermittent irradiation includes five dark or post polymerization processes (eq 3), whereas continuous irradiation includes only one postpolymerization. As a result, ξ during time-intermittent polymerization is markedly higher than ξ during continuous polymerization for the same time of irradiation (Table 1).³⁰ Additional pulses led to a very small increase of conversion, for example $\xi = 0.85 \pm 0.05$ after 10 pulses.

Within the experimental error of determination, the conversion of monomer measured through heat $\xi = Q/Q_{\text{tot}}$ is the same as ξ measured by IR (Table 1). The k_t/k_p value obtained after 3 s of irradiation and $\xi = 0.5$ is between the k_t/k_p values obtained under time-intermittent irradiation at $N = 1$ and $N = 5$ ($\xi = 0.8$); cf. Table 1. These data provide evidence for the validity of eq 2 with time- (conversion-) dependent k_t and k_p for the analysis of polymerization up to conversion $\xi \approx 0.8$.

The decrease of the k_t/k_p ratio with ξ increase reflects the constraints to bimolecular reactions of macroradicals R_n^* imposed by the increasing viscosity of the medium as polymerization proceeds. Thus, in a nonviscous solvent, k_t/k_p is $\sim 10^3$ at ca. 50 °C.²⁷ Polymerization of neat acrylate results in a significant reduction of reactivity (diffusivity) of R_n^* even after the first short irradiation. Chain termination is diffusion controlled, or it quickly becomes diffusion controlled after the increase in solvent viscosity during polymerization. One can expect that as viscosity increases, both propagation and termination reactions will eventually become diffusion-controlled, so that at high enough viscosity $k_t/k_p \sim 1$. In our experiments we were not able to get k_t/k_p less than 20. It is possible that eq 3 is not at all applicable at high ξ , e.g., at $\xi > 0.8$, such as in our case. A ratio of $k_t/k_p = 32$ was reported in a photoDSC study of polymerization of neat dimethylacrylate (40 °C, $\xi \approx 0.4$).²⁹

3.6. PhotoDSC Investigation of the ITX Photosensitized Polymerization of IBOA. The effect of ITX addition on the heat evolved during polymerization of IBOA initiated by TMDPO was studied, employing different UV-light intensities and monochromatic light λ 385 nm (cf. section 2.2), for a range of concentrations of TMDPO and ITX; cf. section 2.2. PhotoDSC data demonstrated that heat evolved during short-time (0.6 s) UV irradiation of solution TMDPO in IBOA is higher in the presence of ITX. The relative increase of heat in the presence of ITX was found to be 10–100% in our experiments. PhotoDSC experiments with solutions of ITX and IBOA do not result in heat evolution within the experimental error of determination of Q (see Table 1). This result demonstrates that ITX serves as a photosensitizer and not as a photoinitiator. These results, along with the cure monitoring results, show that ITX accelerates the photoinduced polymerization of IBOA.

4. Conclusions

The mechanism of the direct and sensitized photoinitiated polymerization of a model acrylate (IBOA) was investigated by TR EPR, cure monitor, and photoDSC techniques. The photoinitiation system of TMDPO and ITX was of primary interest. TR ESR allowed direct spectroscopic detection of the primary radicals produced by direct and sensitized excitation of photoinitiator (BAPO and TMDPO) and of the secondary radicals produced by addition of primary radicals to monomer. Cure monitoring and photoDSC allowed investigation of the polymerization resulting from the initiation steps by monitoring

an increase in viscosity and by the heat released during polymerization.

TR EPR demonstrates that TX and ITX sensitize decomposition of TMDPO and BAPO into benzoyl- and phosphorus-centered radicals through T–T energy transfer. The polarization of the EPR signals changes from the absorptive (direct excitation in the absence of sensitizers) to E*/A (indirect excitation in the presence of sensitizers). A transfer of both single phase (direct excitation) and hyperfine coupling-dependent polarization of P-centered radicals into spin-adduct with acrylate (sensitized excitation) is observed.

Experiments with cure monitoring and photoDSC demonstrated that addition of ITX accelerates the photopolymerization of IBOA initiated by TMDPO in both direct and sensitized excitations.

The ratio of propagation to bimolecular termination rate constants k_t/k_p was estimated in photoDSC experiments during photopolymerization of IBOA initiated by short light pulses. A significant decrease of k_t/k_p was observed as polymerization proceeds: k_t/k_p decreases from values of ca. 95 at low conversions to values of ca. 20 at a conversion of $\xi \approx 0.8$. Values of ξ obtained with IR spectroscopy and with DSC coincide within an experimental error of ξ determination.

Acknowledgment. This work was supported in part by the MRSEC Program of the National Science Foundation under Award No. DMR-98-09687 and by NSF grant CHE98-12676 to the authors at Columbia University. Dr. Steffen Jockusch is thanked for providing useful and critical comments on the manuscript.

References and Notes

- (1) Rutsch, W.; Dietliker, K.; Leppard, D.; Köhler, M.; Misev, L.; Kolczak, U.; Rist, G. *Prog. Org. Coat.* **1996**, *27*, 227.
- (2) Rist, G.; Borer, A.; Dietliker, K.; Desobry, V.; Fouassier, J. P.; Ruhlmann, D. *Macromolecules* **1992**, *25*, 4182.
- (3) Khudyakov, I. V.; Legg, J. C.; Purvis, M. B.; Overton B. J. *Ind. Eng. Chem. Res.* **1999**, *38*, 3353.
- (4) Sluggett, G. W.; McGarry, P. F.; Koptuyug, I. V.; Turro, N. J. *J. Am. Chem. Soc.* **1996**, *118*, 7367.
- (5) Koptuyug, I. V.; Ghatlia, N. D.; Sluggett, G. W.; Turro, N. J.; Ganapathy, S.; Bentrude, W. G. *J. Am. Chem. Soc.* **1995**, *117*, 9486.
- (6) Jockusch, S.; Koptuyug, I. V.; McGarry, P. F.; Sluggett, G. W.; Turro, N. J.; Watkins, D. M. *J. Am. Chem. Soc.* **1997**, *119*, 11495.
- (7) (a) Fouassier, J. P. *Photoinitiation, Photopolymerization, and Photocuring: Fundamentals and Applications*; Hanser: Munich, Germany, 1995. (b) Allonas, X.; Ley, C.; Bibaut, C.; Jacques, P.; Fouassier, J. P. *Chem. Phys. Lett.* **2000**, *322*, 483.
- (8) Angiolini, L.; Caretti, D.; Corelli, E.; Carlini, C.; Rolla, P. A. *J. Appl. Polym. Sci.* **1997**, *64*, 2247.
- (9) Turro, N. J.; Khudyakov, I. V. *Chem. Phys. Lett.* **1992**, *193*, 546.
- (10) Baxter, J. E.; Davidson, R. S.; Hageman, H. J.; McLaughlan, K. A.; Stevens, D. G. *J. Chem. Soc., Chem. Commun.* **1987**, 73.
- (11) Kamachi, M.; Kuwata, K.; Sumiyoshi, T.; Schnabel, W. *J. Chem. Soc., Perkin Trans. 2* **1988**, 961.
- (12) Tarasov, V. F.; Yashiro, H.; Maeda, K.; Azumi, T.; Shkrob, I. A. *Chem. Phys.* **1998**, *226*, 253.
- (13) Gatlik, I.; Rzedek, P.; Gescheidt, G.; Rist, G.; Hellrung, B.; Wirz, J.; Dietliker, K.; Hug, G.; Kunz, M.; Wolf, J.-P., *J. Am. Chem. Soc.* **1999**, *121*, 8332.
- (14) Adrian, F. J.; Akiyama, K.; Ingold, K. U.; Wan, J. K. S. *Chem. Phys. Lett.* **1989**, *155*, 333.
- (15) Khudyakov, I. V.; McGarry, P. F.; Turro, N. J. *J. Phys. Chem.* **1993**, *97*, 13234.
- (16) As is customary, simulations are presented as weighted sum of different mechanisms contributing to the observed polarization.
- (17) Reliable TR EPR spectra are obtainable at $t_0 \approx 200$ ns after a laser pulse. We present boxcar settings t_s in Figures 1–3. Thus, a spectrum is observed at $t = t_0 + t_s$ after a laser pulse with a certain gate Δt .
- (18) Jaegermann, P.; Lenzian, F.; Rist, G.; Möbius, K. *Chem. Phys. Lett.* **1987**, *140*, 615.
- (19) Jockusch, S.; Turro, N. J. *J. Am. Chem. Soc.* **1998**, *120*, 11773.

- (20) Clancy, C. M. R.; Tarasov, V. F.; Forbes, M. D. E. *Electron Paramagn. Reson.* **1998**, *16*, 50.
- (21) Turro, N. J.; Khudyakov, I. V. *Res. Chem. Intermed.* **1999**, *25*, 505.
- (22) Pohlers, G.; Scaiano, J. C.; Step, E.; Sinta, R. *J. Am. Chem. Soc.* **1999**, *121*, 6167.
- (23) Murov, S. L.; Carmichael, I.; Hug, G. L. *Handbook of Photochemistry*; 2nd ed.; Marcel Dekker: New York, 1993.
- (24) Héberger, K.; Fischer, H. *Int. J. Chem. Kinet.* **1993**, *25*, 913.
- (25) Mizuta, Y.; Morishita, N.; Kuwata, K. *Chem. Lett.* **1999**, 311.
- (26) Moad, G.; Solomon, D. H. *The Chemistry of Free Radical Polymerization*; Pergamon: Oxford, UK, 1995; Chapter 2.
- (27) Beckert, A.; Naumov, S.; Mehnert, R.; Beckert, D. J. *Chem. Soc., Perkin Trans. 2* **1999**, 1075.
- (28) Decker, C. *Polym. Int.* **1998**, *45*, 133.
- (29) Gunduz, N.; Shultz, A. R.; Shobha, H. K.; Sankarapandian, M.; McGrath, J. E. *Polym. Prepr.* **1998**, *39*, 647.
- (30) The ascending portions of a curve of Figure 5b were fit to a linear law. A piece of each ascending curve which corresponded to 5–95% of an ordinate of a curve was analyzed.
- (31) It is assumed that the decay of R_n^* does not depend on a reaction of R_n^* with M. A conversion of M in the dark polymerization during half-life of R_n^* ($t_{1/2} = (k_t[R_n^*])^{-1}$) is $\xi = 1 - 2^{-k_p/k_t}$.
- (32) *Polymer Handbook*, 3rd ed.; Wiley: New York, 1989; Chapter 2.